Eddy Current Influence on the Parameters of Active Magnetic Bearing

Zimon Jan[1,a], Tomczuk Bronislaw[1,b], Wajnert Dawid[1,c]
[1]Opole University of Technology, Department of Industrial Electrical Engineering, Poland
[a]b.tomczuk@po.opole.pl, [b]j.zimon@po.opole.pl, [c]dawid.wajnert@op.pl

Abstract: In this work, a symmetrical 8-pole (AMB8) magnetic bearing has been analyzed. The 3D Finite Element Method (FEM) was used for magnetic field computations and nonlinear boundary problem was investigated. We describe discretization process for the AMB modeling, [1]. The power losses and the force of the magnetic suspension have been calculated.

Keywords: Magnetic Bearing, 3D Field Analysis, Eddy Currents, Integral Field Parameters

Introduction

3D Magnetic field analysis has been used for active magnetic bearings (AMB) parameter estimation. The eddy current phenomenon has been included in the analysis. Magnetic flux, due to eddy currents can generate an additional force vector in the radial direction. At high rotational speed particularly in the case of a solid rotor, eddy currents flow on the rotor surface. Due to this phenomenon, they generate phase-delayed components in the magnetic flux wave distribution with respect to the rotor. This has an influence on a direction for the generated radial force error in AMB.

We have considered a high-speed drive system with the asynchronous motor and the magnetic bearings, settled in one casing. The rated speed and torque of the drive are n=40,000 RPM and T_N=0.065 Nm, respectively. The rotor mass of m=1.2 kg is suspended due to the magnetic force arisen from both main flux, under the bias current of I_b=0.8A, and the additional flux by the control current. For the unstable rotor position, the controller should change all excitation currents so that they is well kept, especially when their rotational speed is close to the critical banding mode [3]. The traditional analytical methods for such calculations are not sufficiently correct [3], [4]. Thus, we adopted the Finite Element Method (FEM) for 3D magnetic field analysis.

Description of the numerical problem

The analyzed AMB construction consists of two main parts: a stator and a rotor. Each of them has been stacked from the silicon sheets. The excitation winding consists of 8 symmetric coils, each with N=40 turns. To receive the bias magnetic flux, the coils were supplied with the bias current of I_b=0.8A. The control winding includes 4 symmetrical coils with N=24 turns. The magnetic core and coils creates four horseshoe electromagnets. Each of them has been stacked from sheets of non-homogeneous and nonlinear material. The sheets of the rotor package are fixed on the solid iron shaft, which creates also the main part of the electric drive rotor. The magnetic field computation is a boundary problem for a nonhomogeneous and nonlinear region. Thus, we constructed a field mathematical model of the magnetic bearing. Including its symmetry, we analyzed only a quarter of the AMB geometry.

The magnetic field excited by the magnetic intensity $\vec{H}_s$ can be described by the elliptic partial differential equations,

$$\nabla^2\vec{T} = j\omega\mu\gamma\left(\vec{H}_s + \vec{T} - \nabla\Omega\right) \tag{1}$$

$$\nabla \bullet (\nabla\Omega) = 0 \tag{2}$$

where $\vec{T}$ and Ω represent the electric vector potential and magnetic scalar one, respectively. The first one, can be used for field analysis of the conducting regions, especially for the regions where we have calculated the eddy current density. The magnetic field intensity $\vec{H}_s$ excited by the coils can be simply obtained from the Ampere law,

$$\oint_l \vec{H}_s \bullet \vec{dl} = \Theta \tag{3}$$

where, Θ are the amperturns of the excitation coils.

We used the FEM method for the solution of the equations (1) and (2). Thus, the values of the potentials have been calculated in each finite element of the region. With the knowledge of them, field density distribution has been determined and the eddy currents have been calculated.

Generally, when the displacement current density can be disregarded, Faraday's law can be written

$$\nabla\times(\gamma^{-1}\nabla\times\vec{H}) = -\frac{\partial\mu\vec{H}}{\partial t} \tag{4}$$

where $\vec{H}$ is the magnetic field intensity. When the well-known T– $\nabla\Omega$ method is applied in the finite element solution of this equation, the $\vec{H}$ -field is split into three components:

$$\vec{H} = \vec{H}_s + \vec{T} - \nabla\Omega \tag{5}$$

Edge elements are well suited for generating basis functions for the "electric vector potential space" (where $\vec{T}$ is approximated), whereas conventional nodal elements give basis functions for the gradient space. The induced current density is expressed by $\vec{J} = \nabla\times\vec{T}$. The approximation of $\vec{T}$ is

$$\vec{T} = \sum T_i\vec{t}_i \tag{6}$$

where are the edge element basis functions T_i is the corresponding degree number of freedom (DOF). Thus, the approximation of $\vec{J}$ is

$$\vec{J} = \sum_i T_i\nabla\times\vec{t}_i \tag{7}$$

Therefore, $\nabla\times\vec{t}_i$ can be regarded as basis functions for $\vec{J}$, so that $\nabla\cdot\vec{J} = 0$.

To calculate magnetic flux density distribution, the potential Ω can be used. Due to the numerical process, the magnetic flux density can be obtained using formulas (8) and (9).

$$\vec{B} = \mu_r(H)\,\mu_0\left[\vec{H}_s - \nabla\Omega\right] \tag{8}$$

$$\vec{B} = -\mu_r(H)\,\mu_0\nabla\Omega \tag{9}$$

Using one-step virtual work formula [1], [2], we obtained the magnetic forces on the AMB rotor. Thus, the stiffness parameters of the bearing have been determined, as well.

Numerical model of the 8-poles AMB

The stator ferromagnetic parts and the laminated track as well as the air gap of 0.2 mm between them constitute the path of magnetic flux. Any steel sheets of the bearing parts have been discretized separately in this boundary problem. Sheets of the stator have a thickness of 0.5 mm. It was assumed that the thickness of isolation between the sheets is 0.025 mm. The rotor lamination is remagnetized twice upon a single revolution. In order to avoid losses in the rotor, it was made from sheet metal of thickness less than the stator. Sheets of the rotor have a thickness of 0.2 mm. It was assumed that the thickness of isolation between the sheets is 0.01 mm.

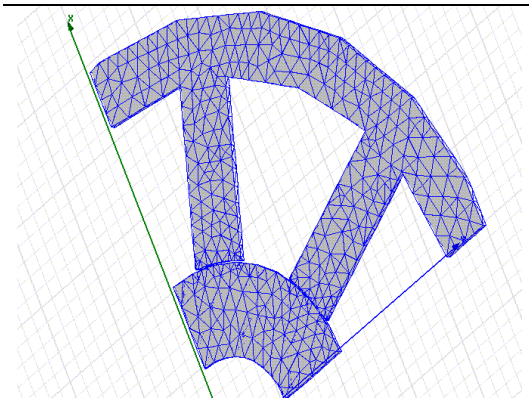

Fig. 1. The discretization mesh of one sheet in the stator and the rotor

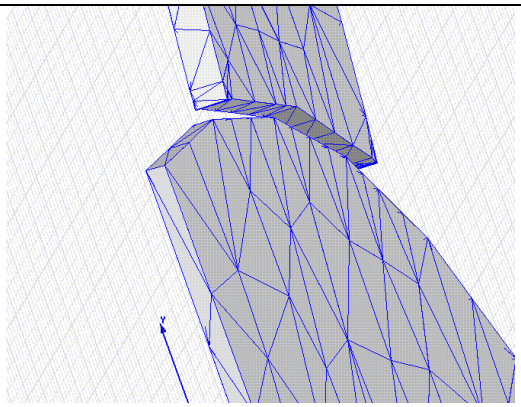

Fig. 2. The zoom of the mesh part at the air gap area

The mesh has been refined in the air gap between the stator and the rotor. The smaller elements of the mesh have been assumed in the pole area, where the high gradient of the magnetic permeability was expected.

a)

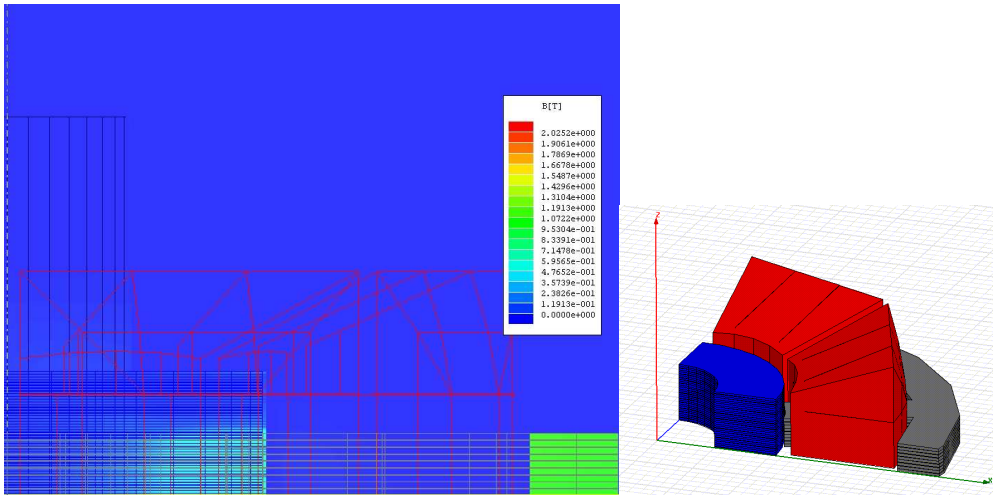

Fig 3a. The distribution of flux density in individual bearing sheets, I_s = 2.5 A. The cross section in the plane XZ

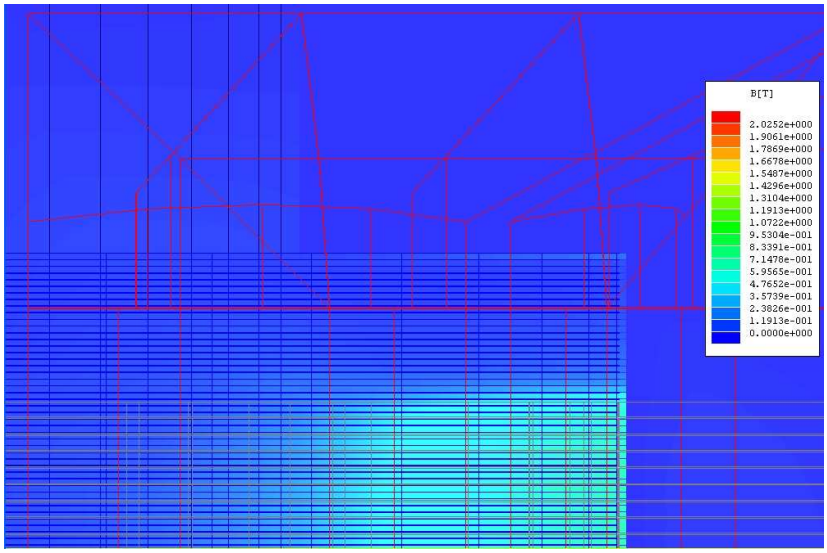

Fig 3b. Flux density in enlarged area of the rotor lamination in individual bearing sheets, I_s=2.5A

In Fig. 3, the magnetic flux density distribution in the iron sheets of the AMB is presented. Figure 3b is an enlarged fragment unit of the flux density map in the rotor packages.

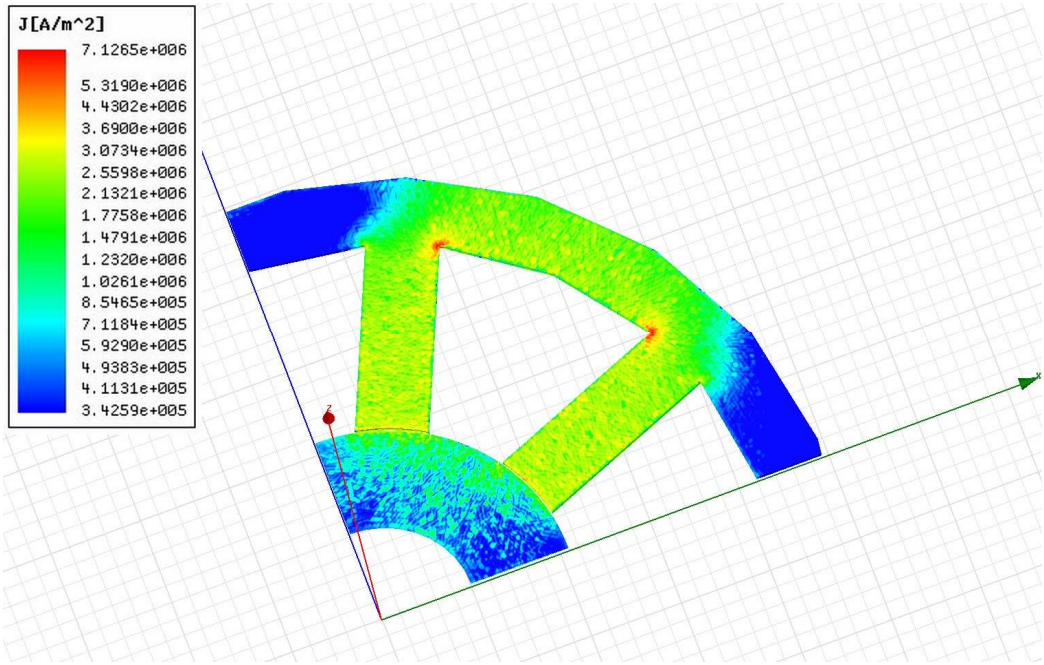

Fig 4. Distribution of eddy current density module for f=500Hz

The highest values of eddy current density are observed in the pole regions of the AMB.Based on the distribution of the eddy current distribution, the losses in the rotor have been computed for different remagnetization frequencies *f* and bias current values. In order to verify the numerical calculations we compared their results with the analytical calculations using the known approximate expression

$$P_w = \frac{1}{6}\gamma\pi^2 g^2 f^2 B^2 V_{Fe} \tag{10}$$

where g denotes thickness of the steel sheets, B is the average flux density in every sheet and V_{Fe} is the volume of the steel.

The results of analytical and numerical calculations of power losses and the magnetic force (which is acting on a bearing shaft) depending on the remagnetization frequency are presented in Fig. 5 and Fig. 6.

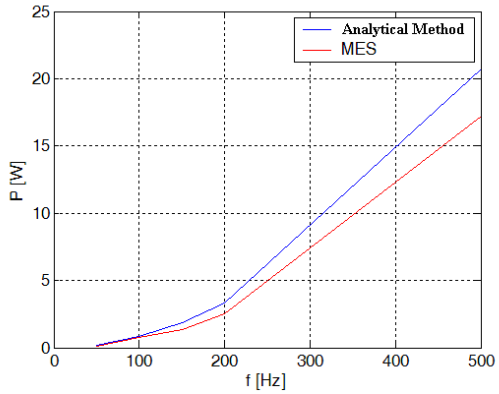

Fig. 5a. Eddy current losses vs. remagnetization frequency, for I_b = 0.48 A

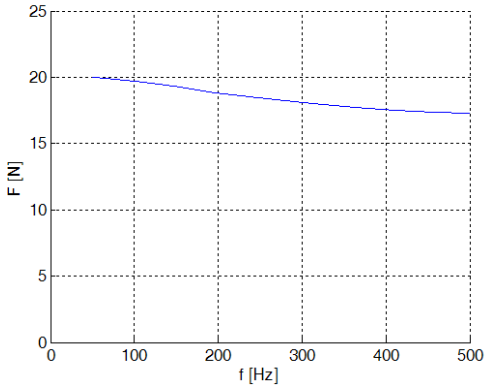

Fig. 5b. Magnetic force vs. remagnetization frequency, for I_b = 0.48 A

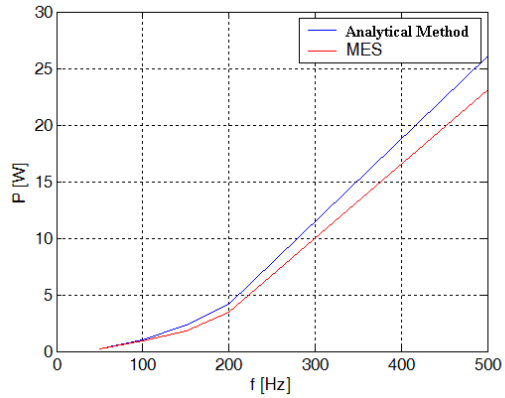

Fig. 6a. Eddy current losses vs. remagnetization frequency, for I_b = 0.8 A

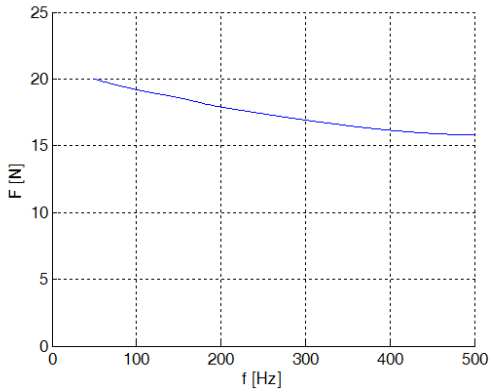

Fig. 6b. Magnetic force vs. remagnetization frequency, for I_b = 0.8 A

Taking into account the eddy current distribution in the AMB, the dependence of the magnetic force (which is acting on the shaft) under variable remagnetization frequency has been designated. Based on numerical results (Fig. 5 and 6), we can see that the magnetic force decrease under higher frequency values by almost 20%. However, the eddy current losses increase very fast for high remagnetization speed.

Conclusions

Measurements were conducted to verify the computed results. In this paper we compared the measured and computed values of the suspension force and we obtained a good agreement. Thus, correctness of the magnetic force and field modeling has been confirmed. The computed eddy current losses were compared with the results of analytical approximation. They seem to be close to roughly analytical calculations. For high rotational speed we can observe the influence of the eddy currents on the magnetic force and stiffness parameters of the AMB. The most important benefit of the computer simulations is that, the different constructions of the AMB are worth trying.

Acknowledgement

Publication co-financed by the NCBiR (National Centre for Research and Development, Poland) under grant No N R01 0026 04.

References

[1] Tomczuk B., Zimon J., Field determination and calculation of stiffness parameters in an active magnetic bearing (AMB), Solid State Phenomena Vols. 147-149, 2009, pp. 125-130
[2] B. Tomczuk, J. Zimon, A. Waindok, Effects of the Core Materials on Magnetic Bearing Parameters", Compumag'09, 22-27.11.2009, Florianopolis, Brasil, pp. 39-40
[3] Schweitzer G., Traxler A., Bleuler H., Magnetlager, Springer Verlag, Heidelberg 1993.
[4] Lei Zhu, Knospe C.R., Maslen E.H., Analytic model for a nonlaminated cylindrical magnetic actuator incl. eddy currents, IEEE Trans. on Mag Vol.41/4, 2005, pp. 1248-1258